7th International Conference on Geotechnical and Geophysical Site Characterization

ISC'7 2024

18-21 June, 2024, Barcelona, Spain

ISC'7
CONFERENCE
BARCELONA
18 - 21 June 2024

Edited by: Marcos Arroyo & Antonio Gens

7th International Conference on Geotechnical and Geophysical Site Characterization.
ISC'7 2024

ISC'7
PLENARY LECTURES

Barcelona, Spain
June 18-21, 2024

A publication of:
International Center for Numerical Methods in Engineering (CIMNE)
Barcelona, Spain

Printed by: Artes Gráficas Torres S.L., Huelva 9, 08940 Cornellà de Llobregat, Spain

TABLE OF CONTENTS

Long-term ERT monitoring data analysis to set slope instability attention thresholds based on water level fluctuations

Regina Bianchi[1], Federica Brambilla[1], Azadeh Hojat[1,2#], Greta Tresoldi[3], and Luigi Zanzi[1]

[1] *Politecnico di Milano, Department of Civil and Environmental Engineering, 20133 Milan, Italy*
[2] *Shahid Bahonar University of Kerman, Department of Mining Engineering, Kerman, Iran*
[3] *LSI LASTEM s.r.l., Settala, Milan, Italy*
[#]*Corresponding author: azadeh.hojat@polimi.it*

ABSTRACT

In this paper, we discuss the results of long-term electrical resistivity tomography (ERT) monitoring of a critical slope located on an important high-speed railway gallery. Data were acquired by a customized ERT system from 24 March 2022 until 31 august 2023 and were analysed with the final objective of defining thresholds of attention for resistivity changes derived from water table fluctuations after heavy rainfalls. This helps the authorities in reducing the hydrogeological risk impacts related to potential slope instabilities triggered by extreme meteorological conditions. In order to continuously observe water level changes, five piezometers were also integrated with the ERT monitoring system which is also accompanied by a meteorological station. All datasets were inverted using a time-lapse algorithm that was optimized to minimize artifacts generated by the subsurface complex geology of the site. Due to the long period considered, seasonal temperature corrections on resistivity values were also explored by calibrating a seasonal model of soil temperature versus depth and evaluating the corresponding effects on the resistivity tomographic maps. Finally, the correlation between resistivity values and piezometric levels was studied by producing scatterplot graphs for a selected subzone of the ERT sections. Based on this analysis, a preliminary threshold of attention was defined.

Keywords: ERT monitoring; time-lapse inversion; hydrogeological risk mitigation; piezometric level.

1. Introduction

Rainfalls are considered as one of the main triggering factors for slope instabilities and landslides. Extreme events such as storms and heavy rainfalls are constantly increasing due to climate changes and it is fundamental to develop efficient systems for real-time monitoring of hydrogeological conditions of hazardous sites. The main demand is to activate early-warning systems in case of imminent risk. In recent years, geophysical techniques and especially electrical resistivity tomography (ERT) method have proved to be useful to be integrated with early-warning strategies of hydrogeological risks (e.g., Chambers et al. 2014, 2022; Hojat et al. 2021; Tresoldi et al. 2019, 2020; Bièvre et al. 2021; Zhang et al. 2021). ERT method, thanks to the dependence of resistivity on soil water content, is specifically an effective solution to monitor variations in the hydrogeological conditions of critical slopes.

The development of customized ERT systems, like the one used in this paper, allows adapting the instrumentation to the specific needs of each site and optimizing the acquisition parameters for each individual project. Moreover, these systems are produced to be permanently installed on site, making it possible to automatically perform remote measurements and to program the desired time intervals between data acquisitions. Measured data are sent to a terminal or directly uploaded on cloud systems where they can be stored, viewed, downloaded and processed.

In this paper, datasets collected in the study site during March 2022-August 2023 are analyzed and discussed with the particular focus on the relationship between resistivity changes and water level fluctuations.

2. The study site

The study site (Fig. 1) is located in central Italy and was selected in order to monitor the stability of the slope over a gallery that covers part of a high-speed railway. The position for permanent installation of the instrumentation was selected after a series of preliminary ERT surveys combined with the information coming from the local authority. The ERT monitoring system was then installed on 15 March 2022 and is still in operation.

The system consists of a geo-resistivimeter installed inside a box and connected to two anti-rodent cables with 48 stainless steel plate electrodes that are placed in a 0.4m-deep trench. The measurement sequence is based on the Wenner configuration with a unit spacing of 3m.

The ERT monitoring system is integrated with a meteorological station powered by a solar panel. This station includes a rain gauge, an air temperature sensor, a soil temperature sensor at 1.5m depth, and a temperature sensor inside the box containing all the electronics to monitor any potential overheating of the instrumentation

that could result in improper functioning. Five piezometers (named S4, S3, S5, S1 and S2, as shown in Fig. 1) were also installed in five stratigraphic boreholes along the ERT profile.

Figure 1. Google view of the study site showing the position of the 48 electrodes (numbered from left to right) of the ERT system and the five piezometers S4, S3, S5, S1 and S2.

2.1. Site stratigraphy

During the preliminary phases, five stratigraphic boreholes were drilled to define the stratigraphy of the site (Fig. 2). This model was then confirmed by observing the corresponding resistivity sections during the monitoring period (an example of which is shown in Fig. 3), which also allowed to obtain a more detailed representation of the specific tendencies of different zones.

It can be noticed both from the stratigraphy and from the resistivity sections that the first 4m of soil are mostly composed by homogeneous conductive materials, although their thickness varies along the profile. Instead, deeper layers show a marked heterogeneity both in the vertical and horizontal direction. In particular:

- The left area (S4) presents an alternation of a silty-clayey sand matrix and some marl blocks; these materials have a low permeability and medium-high resistivity, with typical values ranging between 2000-3000Ωm.
- The middle-left area (S3) is composed by a sandy-loamy soil and stone blocks/calcareous gravels, which are all resistive and mostly low-permeable materials.
- The central area (S5) is characterized by the presence of gravels and sands, which are highly resistive (up to 3000Ωm), but also quite permeable. According to Fig. 3, the resistivity decreases with increasing depth; this is the typical trend during autumn and spring due to the presence of water, while during summer, when piezometric levels are low, resistivities become similar to those of the upper layers.
- The middle-right area (S1) has a thick layer of alteration of chaotic clays and a stratigraphy similar to the region of S4; anyway, resistivity values are very low (usually less than 500Ωm) since the water table is considerably higher than in the left part of the site, fluctuating around 4-5m.
- The right area (S2) has a very similar stratigraphy to the middle-right region, but resistivity values are much higher due to the lower position of the water table, that is always below 8m; according to resistivity sections, this is the area with the highest values during all the monitoring period, arriving at about 6000Ωm during the summer.

The stratigraphic map and the resistivities along the sections are generally similar and they both highlight the presence of different materials with non-homogeneous behaviours. In particular, the area between S5 and S1 is the most conductive due to the presence of water, but resistivity values are higher at depths shallower than the water table; instead, the lateral parts are highly resistive because of their soil composition. In terms of permeability, the central area seems to be the most permeable to rainfalls being the area that shows remarkable drops of resistivity values immediately after rainfall events.

The heterogeneity of the site includes not only the materials, but also the piezometric levels. In fact, the region including S4, S3 and S5 has an average level between 13-15m, while in the right part the water table is higher, reaching about 8-9m in S2 and 4-5m in S1.

The available data from stratigraphy, resistivity maps and piezometers allow to obtain compatible results about the subsurface material and hydrology of the site, which are particularly complex. This fact also strongly influenced the inversion process described later.

3. Data analysis

The ERT system is currently programmed to make two measurements per day, one at 1:00am and one at 1:00pm. A preliminary quality assessment showed that the data acquired during the night are less noisy than those acquired during the day, mainly due to the absence of train passages. Therefore, datasets measured at night were used for the long-term analyses presented in this paper. Further studies were then performed to calibrate the inversion parameters in order to obtain realistic resistivity sections with minimal inversion artifacts (Hojat et al. 2024). The effects of seasonal variations in soil temperature on resistivity data were also modelled to evaluate the necessity for applying appropriate corrections.

3.1. Inversion optimization

Data measured in ERT surveys are not the true resistivity values but the apparent resistivity ones. Each apparent resistivity is a complex function of the true resistivity distribution in the zone influenced by current flow in the subsurface. In order to calculate the real resistivity in the subsurface from the measured apparent resistivity values, an inversion procedure must be applied to the measured data (Loke 2024). A main challenge of geophysical inversions is their inherent ill-posedness, i.e., different model parameters might produce almost the same experimental observations (Aleardi et al. 2022). Apparent resistivity pseudosections were inverted using the Res2dinvx64 software (Copyright © Seequent Systems, Incorporated).

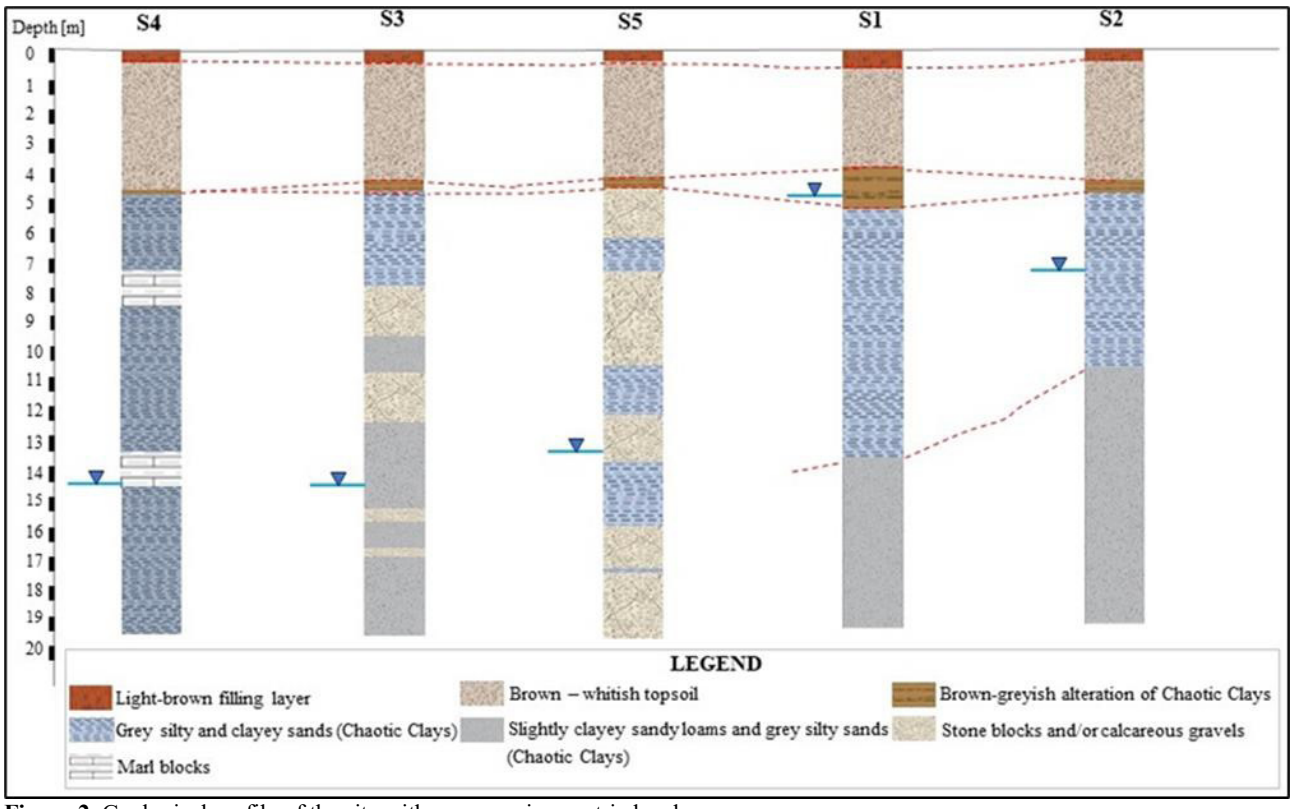

Figure 2. Geological profile of the site with average piezometric levels.

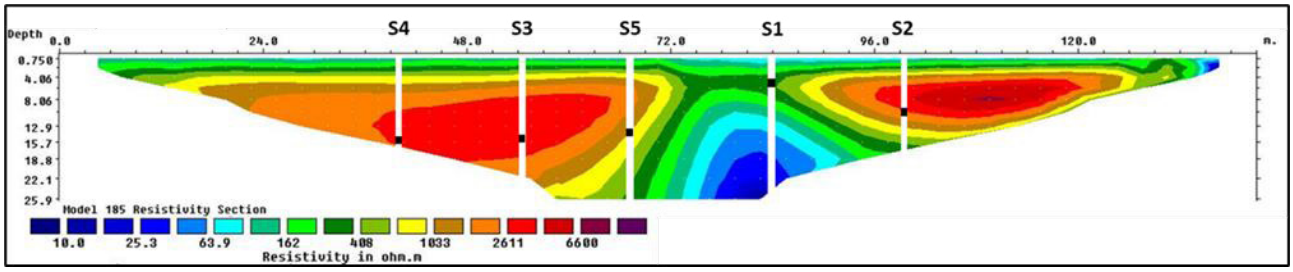

Figure 3. Example of a resistivity section with the position of the 5 piezometers and related groundwater levels.

The study site has a complex geology with both vertical and horizontal variations of materials and layer thicknesses and consequently different soil permeabilities. Moreover, the measured piezometric levels demonstrate very different behaviours along the ERT line. This complex situation resulted in significant inversion artifacts when individually inverting the data. Fig. 4a reports an example of such artifacts. The section shows the difference between two datasets measured with 24 hours of time difference and inverted individually. In this period, a cumulated rainfall of 21.4mm was registered by the rain gauge. Therefore, we expect to observe negative resistivity variations on the whole section. Instead, only the central area of the section follows the expected behaviour, while lateral parts show anomalous increases up to about 20% in resistivity, which is a situation that would typically happen in a drying process. The opposite situation happens when the rainfall stops and the soil starts drying. During dry periods we expect positive resistivity variations on the whole section, but we observed positive variations only in the central zone and negative changes (again artifacts) in the lateral parts.

Hojat et al. (2024) demonstrated that inversion artifacts could be avoided by using a time-lapse inversion algorithm. Their study was focused on several forward modelling simulations of synthetic time-lapse data. Simplified models of the study site were used to explore this problem and study which parameters must be calibrated in order to correctly represent the site. In particular, the optimal condition proposed by Hojat et al. (2024) for this particular site was the application of a smooth (L2 norm) constraint for spatial roughness and a robust/blocky (L1 norm) constraint for temporal roughness, along with a time-lapse damping factor of 5. The robust/blocky inversion constraint for spatial roughness gives optimal results for models with sharp transitions in subsurface resistivity values while the smooth inversion method results in an inversion model with smooth variations in the subsurface resistivity (Loke et al. 2003). The smooth changes and the robust/blocky changes for temporal roughness constraint respectively ensures that time changes in the resistivity values of the

corresponding model blocks are smooth or blocky. Finally, the temporal damping factor controls the relative importance given to minimize the difference between models at different times.

The time-lapse inversion algorithm with the mentioned parameters was thus applied to datasets shown in Fig. 4a and the result is illustrated in Fig. 4b, now allowing us to correctly follow the real changes in the site. We can now observe that the entire area has negative or null resistivity variations, with larger changes located in the middle of the section and in the shallow zone. Such changes are reasonable because this central zone has a higher permeability compared to lateral parts.

3.2. Temperature correction

The scientific literature reports numerous studies showing that soil temperature can significantly affect its resistivity (e.g., Hayley et al. 2007, 2010; Chambers et al. 2014). During long-term monitoring projects, the soil temperature undergoes a series of seasonal variations that, depending on the site morphology, can affect the resistivity values down to 5m or deeper.

In order to account for the effect of air temperature variations on soil temperatures, it is first necessary to define a soil temperature model predicting soil temperatures at different depths (Brunet et al. 2010; Chambers et al. 2014; Bièvre et al. 2021). In our study, soil temperature data were available at the depth of 1.5m and these measurements along with air temperature values were used to calibrate the parameters of Eq. (1), which defines a sinusoidal model for temperature variations, T(z,t), at time (t) and depth (z):

$$T(z,t) = T_{mean(air)} + Ae^{-\frac{z}{d}} sin(\omega t + \Phi - k\frac{z}{d}) \quad (1)$$

where $T_{mean(air)}$ is the mean annual air temperature, A is the maximum variation from the mean temperature, ω is the angular frequency ($\omega = 2\pi/365$) and Φ is the phase. We first applied Eq. (1) to air temperature data where the depth z is assumed to be zero and we obtained A and Φ. Then, d (the characteristic penetration depth of temperature variations) and k were calibrated using soil temperature data at depth z=1.5m. The obtained parameters are reported in Table 1.

Using the calibrated parameters for the study site, a maximum difference of 4.7°C was obtained between the measured and modelled soil temperature values. The largest differences were observed during December 2022 and February 2023. The reason is that these months were particularly warm compared to typical winter conditions. However, the calibrated model fits well for most of the monitoring period and we used it for subsequent analyses.

After calibrating the necessary parameters, the model described in Eq. (1) was applied to all the depths defined in the model layers of inverted resistivity sections. The results showed that the seasonal fluctuations of temperature in the study site can be observed down to about 10m, while temperature values remain basically stable for deeper layers.

Table 1. Parameters of Eq. (1) calibrated for the monitoring period.

Parameter	Calibrated value
$T_{mean(air)}$ [°C]	16.2
A [°C]	12.5
Φ [rad]	-0.5
d [m]	4.5
k [-]	0.8

Having all the temperature models, it was possible to correct the inverted resistivity values for seasonal effects using Eq. (2) (Hayley et al. 2007). The equation allows to transform resistivity values measured at a certain temperature (T) to the values that would be measured at a reference temperature (T_{mean}, that in our case is equal to 16.2°C). This can be done knowing that the α coefficient describes 2% changes in resistivity for 1°C changes in temperature.

$$\rho_{T_{mean}} = \rho_T[1 + \alpha(T - T_{mean})] \quad (2)$$

The resistivity values of different model layers (i.e., at different depths) were thus corrected according to Eq. (2). In order to evaluate the magnitude of temperature effects, we can analyse the maximum percentage correction applied to each layer. The first three resistivity layers down to about 4m registered maximum corrections larger than 10%. The corrections then remarkably decrease with depth. In particular, for layers deeper than 10.4m, the effects were smaller than the estimated background noise (about 2%) and consequently they could be ignored.

The analysis demonstrated that temperature effects for this site are not negligible, in particular in the first three layers of the resistivity model. As a result, all the data were corrected for temperature effects, even if some depths considered for the analysis of resistivity and piezometric levels were affected only marginally by this phenomenon.

3.3. Rainfalls and piezometric levels

The ultimate goal of this study was to use time-lapse ERT as a methodology to monitor the slope behaviour under different hydrological conditions, performing a long-term analysis of resistivity in relation to rainfalls and variations of the piezometric levels.

As described in paragraph 2.1, there is a different site behaviour between the left part, where S4 and S3 piezometers are located, and the central and right regions, where S5, S1 and S2 piezometers are located. On the left and right side of the ERT profile, resistivity values are high due to the massive presence of highly compacted clays and stone blocks. Such composition also results in slow response of this part to rainfalls. Instead, the central region has a faster response to rainfalls and registers lower resistivities, especially in the zone between piezometers S5 and S1. This is related to the soil being mainly composed of sands and gravels. Deeper layers, instead, are much less sensitive to rainfalls because they are already saturated by groundwater.

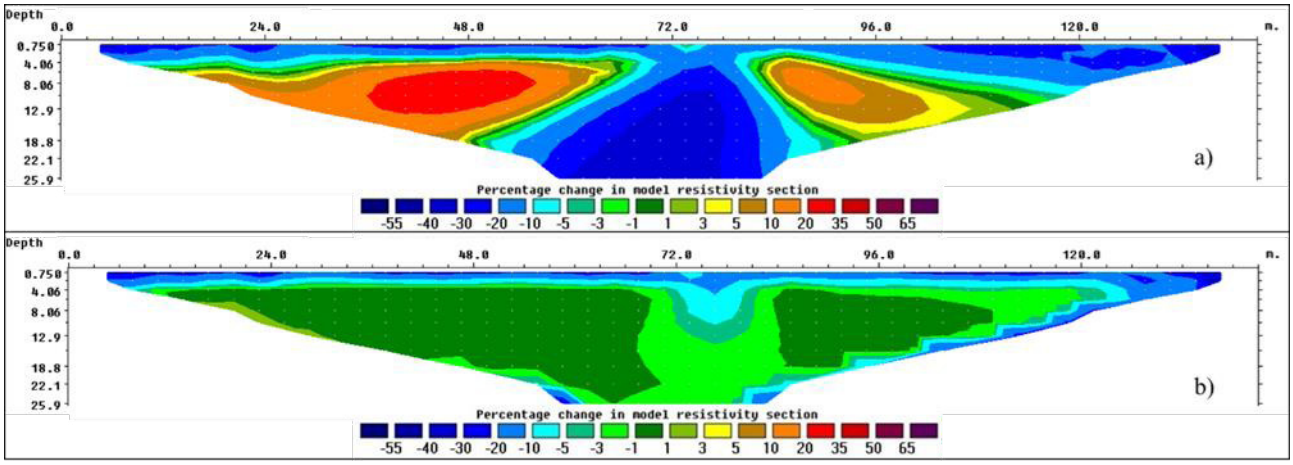

Figure 4. An example of percentage resistivity changes after a rainfall event for the data measured on 4 and 5 November 2022, obtained with (a) individual inversion, and (b) time-lapse inversion with optimal parameters.

The other difference between the two parts of the site is the piezometric level. Groundwater levels observed by piezometers S4, S3 and S5 are considerably deeper than the ones recorded by S1 and S2. Moreover, each piezometer demonstrated to have a different reaction to rainfalls. Out of the five, S5 turned out to be the most sensitive one, being the only that reacts well to both low-intensity and high-intensity meteorological events. This happens due to its position in the central area of the site, which has the highest soil permeability.

As a result, the surroundings of S5 were selected for conducting the most detailed analyses.

3.4. Resistivity and water level correlation

Considering the site complexity in terms of stratigraphy and water levels, the correlation between resistivity values and piezometric data could not be analysed over the whole ERT sections. It was necessary to define small sub-zones near piezometers with vertical extensions including water level fluctuations. Having seen that S5 is the most reactive one, it was chosen as a focus for this study. A sub-region called RS5 was defined in the surroundings of the piezometer, at depths compatible with the average measured water level. RS5 is positioned between 66m and 72m along the ERT profile and extends in depth from 11.6m to 14.2m.

Fig. 5 shows the average inverted resistivity values within the RS5 region for all the monitoring period, with respect to cumulated rainfalls in 24 hours (top) and water levels measured in S5 (bottom). The RS5 zone remains partially saturated for almost the entire period, with the exception of the last two weeks of July 2023. Average resistivity values are higher during summer periods due to the scarcity of rainfalls, which also remarkably lowers the water levels; also, the main soil components of the area are gravels and sands, which can register resistivity values up to few thousands of Ωm when they are dry. Resistivities decreased after rainfalls occurring between September and November 2022, stabilizing afterwards in a range between 500Ωm and 1000Ωm. Resistivity values also decreased in presence of rainfalls during the subsequent winter and spring seasons, although the variations were much smaller. This happens probably due to the difficulty of soil to dry at lower temperatures, which causes a prolonged saturation and reduces the resistivity response.

Although for this reason the piezometer is more sensitive than resistivity to winter and spring rainfalls, on the whole the general trends of the average resistivity values in RS5 are compatible with changes in the piezometric levels observed in S5. In order to further explore this relationship, a scatter plot of the daily pairs of average resistivity values and water levels was created (Fig. 6). Different time periods are highlighted with different colours in order to facilitate observing the different trends associated to the dominant meteorological and seasonal conditions.

Two main trends can be distinguished on Fig. 6. The first trend covers the data measured in the spring and summer 2022, plus summer 2023. These data, positioned in the lower part of the scatter plot, are characterized by low water levels, given by scarce rainfalls and high resistivity values ranging from 1000Ωm to about 3000Ωm, given by the dry gravels and sands composing the soil. Resistivity has a good sensitivity to water level variations, as represented by the gentle slope of this part of the scatter plot. However, the data measured during 26 August-25 September 2022 follow a peculiar trend. Although an increase in piezometric levels is observed in this period, no proportional decrease in resistivity values is recorded. This might be due to an instrumental problem that occurred during a storm in mid-August 2022 and resulted in a gap of 10 days in collecting piezometric and temperature data. This gap in data acquisitions is clearly visible in Fig. 5 where piezometric data between 16 and 25 August 2022 are missing. The sensors returned to normal functioning after this event but it is not excluded that some errors persisted for a while.

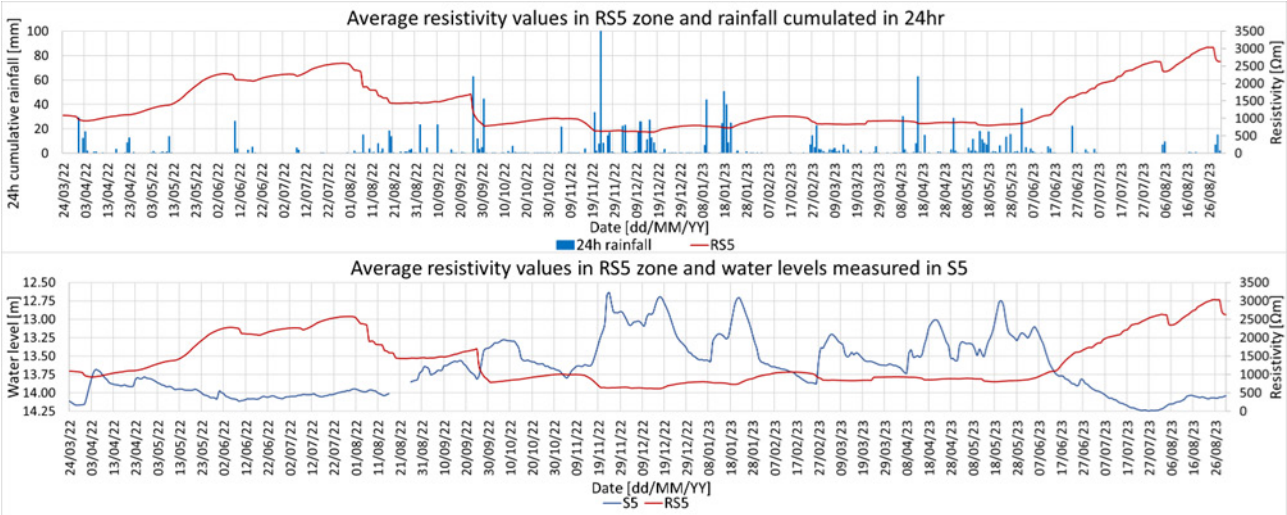

Figure 5. Average inverted resistivity values in the RS5 area compared to rainfalls cumulated in 24hr (top) and water levels measured in S5 (bottom).

The second main trend that can be distinguished on the scatter plot covers the data from autumn 2022 to mid-June 2023 and is positioned in the upper-left part of the graph. Prolonged and moderate-to-abundant rainfalls happened in this period, resulting in rising of water levels and accordingly, decreases in resistivity, given by both the higher soil water content and the rise of the water table that made about 60% of the RS5 region saturated. The slope of the scatter plot is much more pronounced than in the spring-summer period, confirming that resistivity is less sensitive to water level variations.

It is possible to observe that the transition between the two main trends indicated above is well marked by the intersection of the two red lines plotted on Fig. 6. The values individuated by these lines are 13.6m for water level and 960Ωm for resistivity and define the border between the dry period and the period where water levels rise to their peak values. These values can therefore serve as a potential initial pair of thresholds to be used as an attention marker.

Previous studies have tried to model the relationship between resistivity and soil water content (Tresoldi et al. 2019), or resistivity and soil moisture (Chambers et al. 2014), or resistivity and water saturation (Brunet et al. 2010) by using mathematical equations with empirical parameters. In our study, no data are currently available for the actual soil water content, but in order to explore the soundness of a preliminary empirical model, we decided to use the water levels measured by the S5 piezometer as a proxy of the soil saturation. The scatter plot obtained in Fig. 6 and the fitting empirical curve (dashed black curve) seem consistent with the results obtained by other research groups (Brunet et al. 2010; Chambers et al. 2014).

The empirical curve to fit the data was defined by adapting the equation proposed by Waxman and Smits (1968). This equation has been widely used by other researchers (Gunn et al. 2015; Onovughe and Sofolabo 2016). As mentioned, the application of Waxman and Smits equation to our data is somehow questionable because of approximating the missing soil saturation values using piezometric level data. However, the resulting curve seems to adapt well to the available data, demonstrating that, for this specific case study, the Waxman and Smits model is probably appropriate and that the water level data can be considered as an acceptable approximation of soil saturation. This does not exclude the fact that the availability of water saturation data would surely improve the results.

The results obtained in this section confirmed the correlation between resistivity changes and water level variations. In particular, the relationship between the two quantities is roughly described by the Waxman and Smiths equation, which provides a suitable model for further studies.

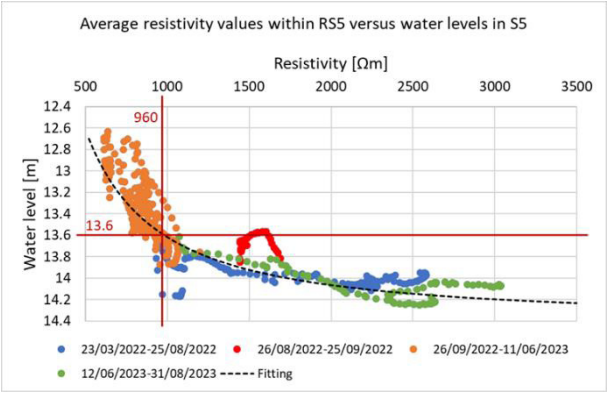

Figure 6. Scatterplot showing the correlation between the average resistivity values within the RS5 zone and the piezometric levels observed in S5. Red lines mark the identified thresholds and the dashed black curve represents a fitting curve inspired by the Waxman and Smits equation.

Furthermore, the scatter plot analysis helped identify the seasonal behaviour of resistivity and piezometric levels, delineating two distinct periods:

- The dry season (late spring/summer), characterized by high resistivities and deep water levels due to the scarcity of rainfall.

- The wet season (autumn/winter), characterized by medium-abundant rainfalls and consequently shallow water levels and low resistivities.

The wet season is the most critical in terms of hydrogeological risk, because the high soil water contents determine higher hydrogeological stress on the slope. The individuated thresholds of 13.6m for water level depth and 960Ωm for resistivity are related to this critical period of the year. This pair of values defines a starting point for more specific analyses aimed at refining such values and integrating/calibrating them with geological/geotechnical models of the site behaviour under different hydrogeological conditions.

4. Conclusions

The analyses presented in this paper showed the efficacy of permanent ERT systems for monitoring a site subject to hydrogeological risk. The importance of optimizing inversion algorithms in presence of geological complexity was demonstrated, finding suitable parameters in order to minimize inversion artifacts. We also explored the impact of seasonal variations of soil temperature at different depths on the resistivity maps. The calibrated soil temperature model for the study site showed that the effects are significant down to about 5-7m. Finally, the response of the five piezometers to rainfalls and the correspondent resistivity response were studied. Out of all, S5 was the most relevant piezometer, and was chosen for deeper analyses of a subzone defined in its sorroundings. An anticorrelation between resistivity and piezometric levels was found inside the RS5 region, and a mathematical relationship was established using Waxman and Smits equation as a model. Despite the partially improper application, the relationship was able to well represent the data, obtaining a suitable model for future analyses.

The results achieved, in particular the resistivity-water level relationship and the provisional thresholds, defines an important starting point for further exploration. These results should be integrated with the information about site geology and with the results coming from laboratory tests and from ERT sections. All of these sources would make possible to refine and update the site model, which could be analyzed with geotechnical softwares to determine the physical conditions that may compromise the stability of the slope, resulting in high hydrogeological stress. Based on that, new resistivity/piezometric thresholds could emerge, establishing the new alarm conditions for the early warning system.

Acknowledgements

The ERT monitoring system is developed by LSI LASTEM s.r.l. with scientific support of Politecnico di Milano. Inversion of ERT data was generated using Seequent Software Res2dinvx64 (Copyright © Seequent Systems, Incorporated).

References

Aleardi, M., Vinciguerra, A., Stucchi, E., Hojat, A. “Probabilistic inversions of electrical resistivity tomography data with a machine learning-based forward operator”, Geophysical Prospecting, 70 (5), pp. 938-957, 2022, https://doi.org/10.1111/1365-2478.13189

Bièvre, G., Jongmans, D., Lebourg, T., Carrière, S. “Electrical resistivity monitoring of an earthslide with electrodes located outside the unstable zone (Pont-Bourquin landslide, Swiss Alps)”, Near Surf Geophys, 19(2), pp. 225-239, 2021, https://doi.org/10.1002/nsg.12145

Brunet, P., Clément, R., Bouvier, C. “Monitoring soil water content and deficit using Electrical Resistivity Tomography (ERT) – A case study in the Cevennes area, France”, Journal of Hydrology, 380(1-2), pp. 146-153, 2010, https://doi.org/10.1016/j.jhydrol.2009.10.032

Chambers, J. E., Gunn, D. A., Wilkinson, P. B., Meldrum, P. I., Haslam, E., Holyoake, S., Kirkham, M., Kuras, O., Merritt, A., Wragg, J. “4D Electrical Resistivity Tomography monitoring of soil moisture dynamics in an operational railway embankment”, Near Surf Geophys, 12(1), pp. 61-72, 2014, https://doi.org/10.3997/1873-0604.2013002

Chambers, J., Holmes, J., Whiteley, J., Boyd, J., Meldrum, P., Wilkinson, P., Swift, R., Harrison, H., Glendinning, S., Stirling, R., Huntley, D., Slater, N., Donohue, S. “Long-term geoelectrical monitoring of landslides in natural and engineered slopes”, The Leading Edge, 41(11), pp. 742-804, 2022, https://doi.org/10.1190/tle41110768.1

Gunn, D. A., Chambers, J. E., Uhlemann, S., Wilkinson, P. B., Meldrum, P. I., Dijkstra, T. A., Haslam, E., Kirkham, M., Wragg, J., Holyoake, S., Hughes, P. N., Hen-Jones, R., Glendinning, S. “Moisture monitoring in clay embankments using electrical resistivity tomography”, Constr Build Mater, 92, pp. 82-94, 2015, https://doi.org/10.1016/j.conbuildmat.2014.06.007

Hayley, K., Bentley, L. R., Gharibi, M., Nightingale, M. “Low temperature dependence of electrical resistivity: Implications for near surface geophysical monitoring”, Geophys Res Letters, 34(18):L18402, 2007, https://doi.org/10.1029/2007GL031124

Hayley, K., Bentley, L. R., Pidlisecky, A. “Compensating for temperature variations in time-lapse electrical resistivity difference imaging”, Geophys, 75(4):WA51-WA59, 2010, https://doi.org/10.1190/1.3478208

Hojat, A., Ferrario, M., Arosio, D., Brunero, M., Ivanov, V. I., Longoni, L., Madaschi, A., Papini, M., Tresoldi, G., Zanzi, L. “Laboratory studies using electrical resistivity tomography and fiber optic techniques to detect seepage zones in river embankments”, Geosciences, 11(2):69, 2021, https://doi.org/10.3390/geosciences11020069

Hojat, A., Zanzi, L., Tresoldi, G., Loke, M.H. “Forward modelling simulations to remove inversion artifacts from ERT monitoring data measured on a slope with complex geology”, under review: Near Surf Geophys, 2024.

Loke, M.H., Acworth, I., Dahlin, T. “A comparison of smooth and blocky inversion methods in 2D electrical imaging surveys”, Exploration Geophysics, 34(3), pp. 182-187, 2003, https://doi.org/10.1071/EG03182

Loke, M.H. “Tutorial: 2-D and 3-D electrical imaging surveys”. Available at: http://geotomosoft.com, accessed: 18/04/2024.

Onovughe, E., Sofolabo, A. “Saturation modelling: using the Waxman-Smits model/equation in saturation determination in dispersed shaly sands”, Journal of Multidisciplinary Engineering Science and Technology, 3, ISSN:2458-9403, pp. 4985-4992, 2016. Available at: https://www.jmest.org/wp-content/uploads/JMESTN42351620.pdf, accessed: 09/04/2024.

Tresoldi, G., Arosio, D., Hojat, A., Longoni, L., Papini, M., Zanzi, L. “Long-term hydrogeophysical monitoring of the internal conditions of river levees”, Eng Geol, 259:105139, 2019, https://doi.org/10.1016/j.enggeo.2019.05.016

Tresoldi, G., Hojat, A., Zanzi, L. “G.RE.T.A. installations for real-time monitoring of irrigation dams and canals”,

Procedia Environmental Science, Engineering and Management, 7 (2), 271-276, 2020. Available at: https://hdl.handle.net/11311/1160453, accessed: 09/04/2023.

Waxman, M. H., Smits, L. J. M. “Electrical conductivities in oil-bearing shaly sands”, Soc Petrol Eng J, 8 (2), pp. 107-122, 1968, https://doi.org/10.2118/1863-A

Zhang, Z., Arosio, D., Hojat, A., Zanzi, L. “Reclassification of microseismic events through hypocentre location: case study on an unstable rock face in Northern Italy”, Geosciences, 11 (1), 37, 2021, https://doi.org/10.3390/geosciences11010037